

# Towards a new tool for the indirect detection of Dark Matter : building of a SuSy spectrum generator based on micrOMEGAs

Pierre Brun<sup>1</sup>

## Abstract

*In the quest for indirect signals from dark matter annihilation, powerful computation codes are required. I report here a new code based on micrOMEGAs devoted to the analysis of such signals in term of Supersymmetry. It computes gamma rays and positrons fluxes in a general SuSy model, as well as the other charged cosmic rays and neutrinos source terms. This work aims to propose an alternative to the DarkSUSY code by providing inclusive signals from SuSy for dark matter indirect searches. Therefore it can be used for sensitivity studies and data analysis.*

## 1 Supersymmetric dark matter

### 1.1 Supersymmetry and cosmology : the micrOMEGAs code

The Standard Model of particle physics describes two distinct families, bosons and fermions as interaction and matter particles respectively. The integer and half-integer spins can be merged in a unified model if one assumes that a symmetry exists between those two sectors, this is the purpose of Supersymmetry (SuSy). In addition to this aesthetic issue, SuSy can solve some of the Standard Model limitations, such as the stability of the Higgs boson mass as regard to radiative corrections, the unification of forces or the understanding of the electro-weak symmetry breaking mechanism. Since no SuSy particle has ever been detected, it must be that the symmetry is broken at today's reached scales, and partners are heavier than the standard particles. Furthermore, assuming the conservation of a new quantum number called R-parity, SuSy predicts the existence of relic particles from the Big-Bang, these are *stable, neutral, weakly interacting, massive and non baryonic* (WIMP's). When it has these characteristics, the Lightest SuSy Particle (LSP) is a good candidate for dark matter. This possibility is very interesting since WMAP measurement of the cosmic microwave background anisotropies point out that there must be a large amount of non baryonic dark matter in our Universe. These measurements, in addition to the observation of type Ia supernovae, large scales structures features and constraints from Big-Bang nucleosynthesis give the following picture of our Universe content [2]:

- The universe is globally flat, with  $\Omega_{tot} = 1.02 \pm 0.02$ .
- The major part of the energy is under the form of a cosmological constant  $\Omega_{\Lambda} = 0.73 \pm 0.04$ .

---

<sup>1</sup>Laboratoire d'Annecy-le-vieux de Physique des Particules, CNRS/IN2P3/Univ. de Savoie, brun@lapp.in2p3.fr

- The matter component is  $\Omega_{matter} = 0.27 \pm 0.04$  and is 84% non baryonic ( $\Omega_{baryons} = 0.044 \pm 0.004$ ).

`micrOMEGAs` purpose is to accurately compute the relic abundance in a general SuSy model [3] (namely the Minimal Supersymmetric Standard Model, MSSM). To do so, one has to solve the Boltzmann equation:

$$\frac{dn}{dt} = -3Hn - \langle \sigma v \rangle (n^2 - (n^{eq})^2) \quad (1)$$

Where  $n$  is the number density of relic particles,  $\langle \sigma v \rangle$  their annihilation cross section and  $H$  the Hubble constant. Basically this equation indicates that the annihilation rate has to be balanced against the expansion of the Universe, leading to a freeze-out of the LSP. Figure 1 shows how this freeze-out occurs, we can see the evolution of the co-moving wimp density. In the first part, the particles interact sufficiently one with another to make the LSP annihilate, and the LSP density goes down. At a particular temperature, the Universe expands so that the Hubble radius get greater than the mean interaction length. From this moment, the annihilation rate is very low and the relic particles density remains constant.

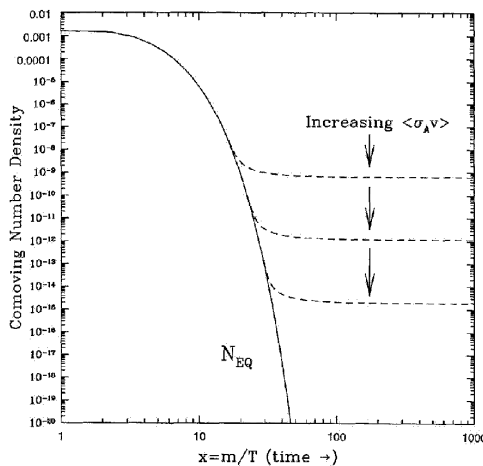


Figure 1: Evolution of the co-moving wimp density with temperature

It happens that some particles have a mass close to the LSP’s mass and then contribute to the decrease of the LSP density, these processes are the so-called *coannihilations* [4]. In that case one has to replace  $\langle \sigma v \rangle$  in eq. 1 by a sum over all coannihilation channels:

$$\frac{dn}{dt} = -3Hn - \sum_{i,j=1}^N \langle \sigma_{i,j} v_{i,j} \rangle (n_i n_j - n_i^{eq} n_j^{eq}) \quad (2)$$

One great performance of `micrOMEGAs` is to dynamically include -when they are relevant- all possible coannihilation channels. The total number of processes that can be involved is about 3000.

## 1.2 Supersymmetry breaking

Once “supersymmetrized”, the Standard Model becomes the Minimal Supersymmetric Standard Model (MSSM). if SuSy was effective, Sparticles would have the same mass as the corresponding particles. Superpartners have never been observed and it must be that SuSy is a broken symmetry. Then one has to parameterize the breaking by introducing terms in the Lagrangian that explicitly break SuSy. This breaking imposes the introduction of over 100 free parameters. In order to make physical predictions, one can fix them or assume a model for

SuSy breaking that generates these soft SuSy breaking terms. In this note, we will work in two SuSy breaking models frameworks :

- Minimal SuperGRAvity, in which SuSy is broken via gravitationnal interaction. In the mSUGRA model, all physical quantities can be derived from 5 parameters specified at the Planck scale, these are :
  - $m_0$ : common scalar mass
  - $m_{1/2}$ : common fermion mass
  - $A_0$ : universal trilinear couplings
  - $tg(\beta)$ : ratio of the neutral Higgs vacuum expected values
  - $sgn(\mu)$ : sign of the Higgs mass parameter  $\mu$
- Anomaly Mediated SuSy Breaking, in which SuSy is broken via the super-Weyl anomaly effects [5] In AMSB, 4 Planck scale parameters are enough to describe the MSSM :
  - $m_0$ : common scalar mass
  - $m_{3/2}$ : gravitino mass
  - $tg(\beta)$ : ratio of the neutral Higgs vacuum expected values
  - $sgn(\mu)$ : sign of the Higgs mass parameter  $\mu$

In those frameworks, the LSP is the lightest neutralino  $\tilde{\chi}_1^0$  (or  $\chi$ ), a mixing of gauge bosons partners. In this note only mSUGRA and AMSB are considered, but the code also allows to work in the Gauge-Mediated SuSy Breaking scenario.

### 1.3 Cosmological constraints on mSUGRA

The initial goal of micrOMEGAs is to compute accurately the relic density, and compare it to cosmological measurements thus putting constraints on the parameter space of a given model. To illustrate this, a scan of the parameter space has been performed. On Figure 2, only the WMAP  $4\sigma$  allowed points are plotted in the  $m_0$ - $m_{1/2}$  plane, *i.e.* when the computed thermal relic density satisfies  $0.076 \leq \Omega h^2 \leq 0.148$ . The mass spectrum generator used here is SuSpect [12].

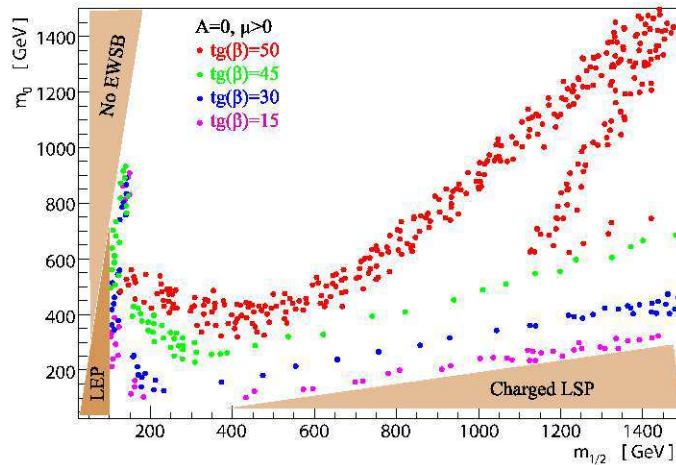


Figure 2: Cosmological constraints on gravity broken SuSy

## 2 AMS02 potential for indirect dark matter searches

AMS02 is a particle physics spectrometer to be placed on the International Space Station for 3 years. The detector allows to measure charged cosmic rays as well as  $\gamma$  ray fluxes in the range of 1 GeV to a few TeV, including particle identification, charge reconstruction, isotopes separation in case of light nuclei [6]. It consists in different specific sub-detectors, with some redundancy in measurements. A Silicon Tracker surrounded by a superconducting magnet provides charge and rigidity, two planes of a time-of-flight detector are used for trigger and direction determination. The Transition Radiation Detector and the Electromagnetic Calorimeter (Ecal) perform e/p separation and energy determination, and a Čerenkov counter measures charge and  $\beta$ .

The principle of indirect search for dark matter is to look for non-standard signals in cosmic spectra, arising from annihilations in the local halo [1]. Such a deviation could be seen in the antimatter to matter ratio for charged cosmic rays (positrons, antiprotons or antideuteron), for which AMS capabilities are very high [6]. Positron signal is of special interest since HEAT experiment has measured an excess which could be explained in terms of a Weakly Interactive Massive Particle (WIMP) annihilation signal [7]. With a background rejection of order  $10^6$ , an acceptance of  $0.04 m^2.sr$  and an energy resolution of 3% in this range, AMS02 is awaited to confirm and precisely measure the positron excess [8]. In the case of  $\gamma$  rays, dark matter is expected to produce an enhancement of diffuse emission from the halo and possibly point-like sources where its density is high. The Galactic center could be such a source, in particular if the halo profile near the supermassive black hole is cusped. Another possibility is to observe a GeV scale line emission, which would give a compelling evidence of the presence of dark matter since no known astrophysical object could be able to produce it. Although originally designed for charged particles detection, AMS02 has high performance in  $\gamma$  rays detection. Two modes allow the spectrometer to perform a measurement whether the photon converts into a  $e^+/e^-$  pair in the upper detector or not. The Tracker is used in the first case and provide good angular resolution ( $0.05^\circ$ ). A specific trigger is used in the other case [9], for which the Ecal allows a 3% energy resolution and a  $1^\circ$  angular resolution. These two complementary ways to detect high energy photons puts AMS02 in great place to perform  $\gamma$  ray astronomy, with high acceptance (of order  $0.09 m^2.sr$ ) and a large sky coverage [10].

## 3 Making micrOMEGAs an event generator

### 3.1 Architecture of the code

The final goal of our package is to predict all indirect signals from SuSy dark matter [11]. The user may choose to work in the general MSSM or with any model constrained at the high scale (such as mSUGRA and AMSB), in that case the first step is to compute the evolution of physical parameters such as masses and couplings from the unification scale to the electroweak scale (EWS) at which cross sections in the halo have to be determined. The evolution from the high scale to EWS is managed here by `SuSpect` [12] which solves the renormalization group equations <sup>1</sup>. All EWS parameters are given to `micrOMEGAs` which computes all cross sections. The former are discussed in next sections. At this point one has to link these final states to observable particles, this task is devoted to `PYTHIA` [13]. It computes the partons hadronization-fragmentation and the decays of unstable particles. For the  $\gamma$  signal the integral of the density over a field of view is computed. The charged particles have to be propagated through the Galaxy from the location of their production to the Earth vicinity, then specific propagation codes are used. In the present note,  $\bar{p}$  and  $\bar{D}$  propagation are not presented, but they will be included in the final version.

---

<sup>1</sup>The results presented here make use of `SuSpect`, but any other RGE code can be used

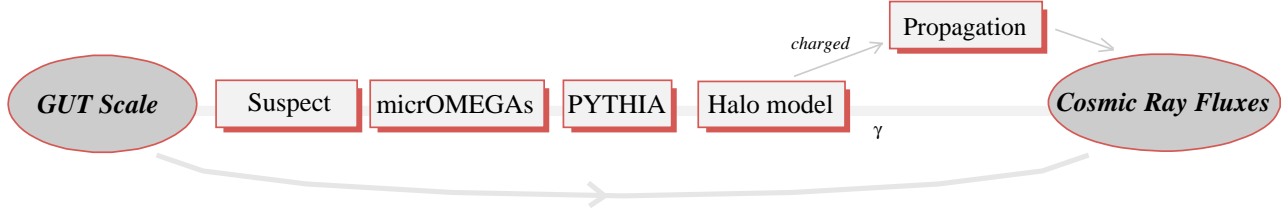


Figure 3: Principle of the code

### 3.2 Fluxes from neutralino annihilations

Dark matter signal in cosmic radiations can be seen either in the matter to antimatter ratio and in  $\gamma$  rays. In this note some results for  $\gamma$  rays and  $e^+$  are presented. Concerning the  $\gamma$  rays from Galactic center, the flux is given by the following expression:

- $\gamma$  rays

$$\Phi_{\gamma}^{Susy} = \frac{dN_{\gamma}}{dSdEdtd\Omega} = \frac{1}{4\pi} \overbrace{\frac{dN_{\gamma}}{dE_{\gamma}} \langle \sigma_{ann} v \rangle}{\text{Particle physics}} \overbrace{\int_{l.o.s.} \frac{\rho_{\chi}^2(r(l_{\psi}))}{2} dl_{\psi}}^{\text{Astrophysics}} \quad (3)$$

Two contributions are present in this equation, one purely astrophysical and the other arising from particle physics. The right part is the density integral along a line of sight, this depends on the modelling of the dark halo. In the other part, from particle physics, the fraction  $\langle \sigma_{ann} v \rangle / m_{\chi}^2$  contains the total annihilation cross section and the neutralino mass, both provided by micrOMEGAs. Here the annihilation cross section has to be computed at the temperature of the halo, whereas for the relic density estimation it was computed at  $T_{freeze-out}$ .  $dN_{\gamma}/dE_{\gamma}$  is the number of  $\gamma$  per unit energy for one annihilation and is computed with PYTHIA (here version 6.123). Each final state giving different  $\gamma$  spectra, this is in fact a sum over all final states :

$$\frac{dN_{\gamma}}{dE_{\gamma}} = \sum_{f.s.} \left[ B_{f.s.} \frac{dN_{\gamma}^{f.s.}}{dE_{\gamma}} \right] \quad (4)$$

As  $\chi$  is electrically neutral, it does not couple to photons, therefore there is no tree level direct  $\gamma$  production. Nevertheless,  $\gamma$  rays arise from the hadronization of the final states partons. A typical example is the decay of  $\pi^0$ 's appearing in the hadronization of a quark/antiquark pair. These processes lead to a continuous  $\gamma$  spectrum. At the 1 loop level,  $\gamma$  lines can be produced via processes such as  $\chi\chi \rightarrow \gamma\gamma, \gamma Z^0$ . The  $\gamma\gamma$  and  $\gamma Z^0$  processes are implemented in our code [15], and give photons at the following discrete energies:

$$\gamma\gamma : E_{\gamma} = m_{\chi} (N_{\gamma} = 2) \quad ; \quad \gamma Z^0 : E_{\gamma} = m_{\chi} \left[ 1 - \left( \frac{m_{Z^0}}{2m_{\chi}} \right)^2 \right] (N_{\gamma} = 1) \quad (5)$$

These processes are of special interest since no known astrophysical source could lead to GeV to TeV  $\gamma$  lines. The observation of such lines would provide a smoking gun signature for the observation of dark matter annihilations in the Milky Way. In this note I present an application of the upcoming tool **SloopS** developed by Boudjema *et al.* that will compute all of the MSSM processes at the 1 loop level. This package will be provided with micrOMEGAs.

- **Positrons**

For the positron signal, the flux is a solution of the propagation equation :

$$\frac{\partial}{\partial t} \frac{dn_{e^+}}{dE_{e^+}} = \vec{\nabla} \cdot \left[ K(E_{e^+}, \vec{x}) \vec{\nabla} \frac{dn_{e^+}}{dE_{e^+}} \right] + \frac{\partial}{\partial E_{e^+}} \left[ b(E_{e^+}, \vec{x}) \frac{dn_{e^+}}{dE_{e^+}} \right] + Q(E_{e^+}, \vec{x}) \quad (6)$$

with the source term :

$$Q(E_{e^+}, \vec{x}) = \frac{\rho_\chi^2(\vec{x})}{2} \frac{\langle \sigma v \rangle}{m_\chi^2} \frac{dN_{e^+}}{dE_{e^+}} \quad (7)$$

Here, micrOMEGAs provides cross-sections and masses, PYTHIA gives the differential  $e^+$  spectrum and a new code is used to solve the propagation equation, developed by Salati *et al.* [14]. The different parts from particle physics and astrophysics are detailed in the following sections.

### 3.2.1 Cross sections and final states

There are 26 possible 2-body tree-level final states for neutralinos self annihilation. These are fermion/antifermion pairs or allowed combinations of gauge and/or Higgs bosons. Each final state will give its own particles yields, with its specific spectral features as we will see in section 4. Therefore it is important to know for a given model or set of parameters which final states will be favored. In the mSUGRA framework, Figure 4 shows the occurrence of some final states ( $b\bar{b}$ ,  $t\bar{t}$ ,  $\tau^+\tau^-$  and  $W^+W^-$ ) in the  $m_0$ - $m_{1/2}$  plane with all other parameters fixed.

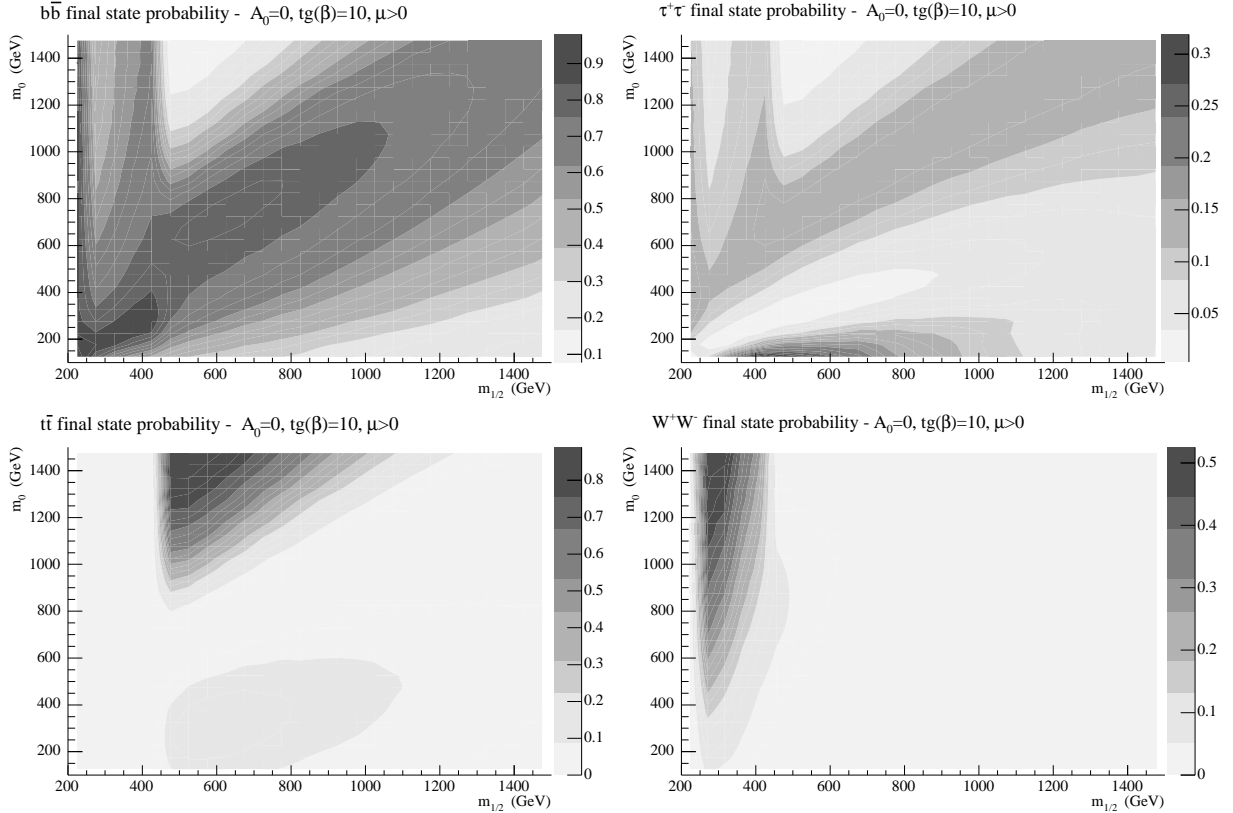


Figure 4: Final state occurrences with  $A_0 = 0$ ,  $\mu > 0$  and  $\tan(\beta) = 10$  in mSUGRA

It appears from Figure 4 that a typical mSUGRA case is the one in which annihilation into a  $b\bar{b}$  pair is dominant, followed by the annihilation into  $\tau\tau$ 's. Some regions of the parameter space lead to an annihilation into  $top$  quarks, with a threshold effect, or into gauge bosons such as  $W$ 's. However, by comparing this figure to Figure 2, one can see that the annihilation into  $W^+W^-$  is not favored by cosmology in the case of mSUGRA. However it will be shown in last section that other supersymmetry breaking scenarios can lead to this final state.

### 3.2.2 Dark halo modelling

The exact local dark matter density is not known and one has to parameterize the halo density profile in order to match the observed gravitational effects. The local dark matter density is in the range  $\rho_\odot = 0.2-0.8 \text{ GeV.cm}^{-3}$  and that does not give information about the density far from the center or near the center. Therefore one has to assume a halo profile that gives the proper local density. The following parametrization is implemented in the code, it allows to describe number of halo profiles (motivated by numerical simulations).

$$\rho_{CDM}(r) = \rho_\odot \left[ \frac{r_\odot}{r} \right]^\gamma \left[ \frac{1 + (r_\odot/a)^\alpha}{1 + (r/a)^\alpha} \right]^{\frac{\beta-\gamma}{\alpha}} \quad (8)$$

In addition to this, any kind of central shape can be specified by hand, this is of special importance if one wishes to test different accretion models onto the central supermassive black hole. Figures 5 and 6 give the most popular halo profiles parameters and shapes, in the case of Navarro-Frenk-White (NFW), Moore and isothermal sphere (see [1] and references therein).

Halo model	$\alpha$	$\beta$	$\gamma$	a (kpc)
Isothermal with core	2	2	0	4
NFW	1	3	1	20
Moore	1.5	3	1.5	28

Figure 5: Halo parameters for three profile types

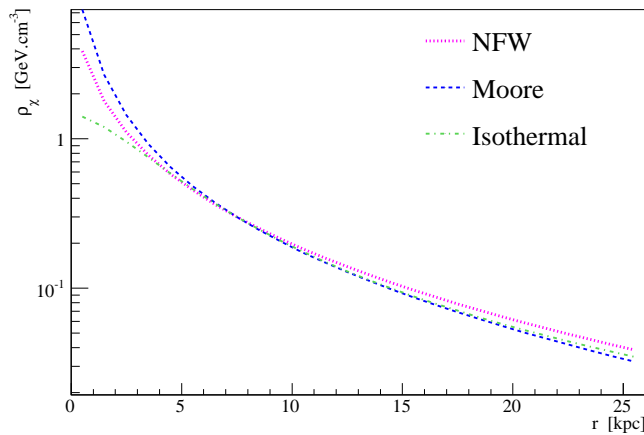


Figure 6: Three examples of halo profiles

This parametrization allows to predict diffuse fluxes from the halo as well as fluxes from the Galactic center. In order to make a prediction for a  $\gamma$  flux from the Galactic center, one has to integrate the signal inside some

solid angle around the direction of the Galactic center. To do so, the code sums all lines of sight contributions such as the ones shown in Figure 7.

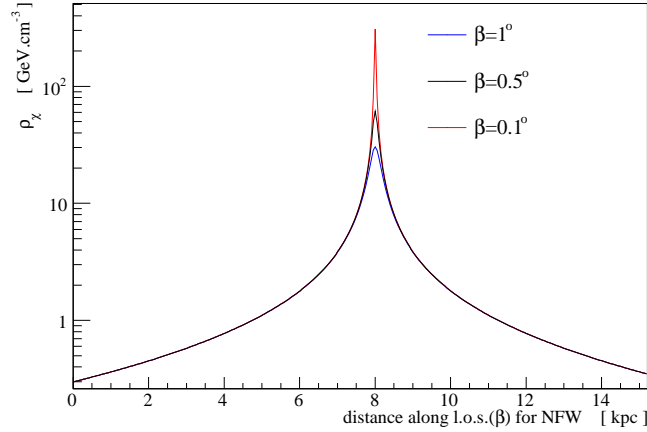


Figure 7: Dark matter density along lines of sight with different angles toward the Galactic center

As an example, the table of Figure 8 show the normalized value of the astrophysical factor  $\langle J \rangle$ , defined as the mean value of  $J$  over a given  $\Delta\Omega$  solid angle. Here  $\langle J \rangle$  is :

$$\langle J \rangle_{\Delta\Omega} = \frac{1}{r_{\odot}^2 \rho_{\odot}^2} \frac{1}{\Delta\Omega} \int d\Omega \int_0^{\infty} \rho_{\chi}^2(r(l_{\psi})) dl_{\psi} \quad (9)$$

Solid angle	$\Delta\Omega = 10^{-3} sr$	$\Delta\Omega = 10^{-5} sr$
Isothermal $\langle J \rangle$	$2.621 \cdot 10^1$	$2.624 \cdot 10^1$
NFW $\langle J \rangle$	$1.291 \cdot 10^3$	$1.346 \cdot 10^4$
Moore $\langle J \rangle$	$1.947 \cdot 10^5$	$1.562 \cdot 10^7$

Figure 8: Astrophysical terms calculation with the package

These figures are obtained with our package, they are in perfect agreement with previous calculations [1]. These figures show that in the case of this observation, a better angular resolution lead to a better observation only in the case of a cuspy halo profile. Indeed for a halo with a flat dark matter distribution in its center, the mean value of the astrophysical factor does not vary when the solid angle is changed.

## 4 First example : $\gamma$ rays from Galactic center in mSUGRA

I wish here to illustrate the use of our package for computing  $\gamma$  spectra from the Galactic center. The astrophysical part used here is a NFW parametrization (the distance to the Galactic center is  $r_{\odot} = 8 kpc$  and the local dark matter density is taken at  $\rho_{\odot} = 0.3 GeV.cm^{-3}$ ). The annihilation rates are integrated inside a  $1^{\circ}$  opening angle cone around the Galactic Center. Then the  $\gamma$  ray flux is given by the following formula :

$$\Phi_{\gamma}^{Susy}(\Delta\Omega) \Delta\Omega = \frac{dN_{\gamma}}{dSdEdt} = \frac{1}{4\pi} \frac{dN_{\gamma}}{dE_{\gamma}} \frac{\langle \sigma_{ann} v \rangle}{m_{\chi}^2} \int_{\Delta\Omega} d\Omega \int_{l.o.s.} \frac{\rho_{\chi}^2(l)}{2} dl \quad (10)$$



As examples, I use two sets of mSUGRA with parameters detailed below. Both points match relic density and accelerator constraints. The first one is used by W. de Boer *et al.* [16] and has the advantage of giving quite a high signal, with a total cross section of order  $10^{-26} \text{ cm}^3 \text{ s}^{-1}$ . The second point gives less flux but a visible line (G' benchmark point [17]). Figure 9 gives some characteristics of the chosen sets of parameters.

Set 1	Set 2
$m_0 = m_{1/2} = A_0 = 500 \text{ GeV}$	$m_0 = 113 \text{ GeV}, m_{1/2} = 375 \text{ GeV}, A_0 = 0$
$tg(\beta) = 50, \mu > 0$	$tg(\beta) = 20, \mu > 0$
$\Omega_\chi h^2 = 0.098$	$\Omega_\chi h^2 = 0.128$
$m_\chi = 206.9 \text{ GeV}$	$m_\chi = 151.5 \text{ GeV}$
$\langle \sigma_{tot} v \rangle = 1.81 \cdot 10^{-26} \text{ cm}^3 \text{ s}^{-1}$	$\langle \sigma_{tot} v \rangle = 6.96 \cdot 10^{-28} \text{ cm}^3 \text{ s}^{-1}$
$\langle \sigma(b\bar{b})v \rangle = 0.87 \times \langle \sigma_{tot} v \rangle$	$\langle \sigma(b\bar{b}) \rangle = 0.58 \times \langle \sigma_{tot} v \rangle$
$\langle \sigma(\tau^+\tau^-)v \rangle = 0.13 \times \langle \sigma_{tot} v \rangle$	$\langle \sigma(\tau^+\tau^-) \rangle = 0.39 \times \langle \sigma_{tot} v \rangle$
$\langle \sigma(\gamma\gamma)v \rangle = 2.10^{-5} \times \langle \sigma_{tot} v \rangle$	$\langle \sigma(\gamma\gamma) \rangle = 0.01 \times \langle \sigma_{tot} v \rangle$
$\langle \sigma(\gamma Z^0)v \rangle = 4.10^{-6} \times \langle \sigma_{tot} v \rangle$	$\langle \sigma(\gamma Z^0) \rangle = 0.001 \times \langle \sigma_{tot} v \rangle$

Figure 9: Main features of the two sets of mSUGRA parameters considered in this part

All the final states cross sections being determined, the  $\gamma$  spectra for each one of them has to be computed. This is done by using `micrOMEGAS` final states as an input to `PYTHIA`, which hadronizes the partons, simulates the jets fragmentation and the decay of all unstable particles that may appear in the hadronization process. Different spectra are obtained for each final states. The final spectra results in weighting these ones with the computed cross sections. The user has different ways to obtain the final signal:

- Monte Carlo generator: The spectrum is produced event by event with a final state random choice according to their probability.
- Weighted channels: Channels are produced separately and then weighted as regard to their cross section.
- Use of tables : A catalog of spectra is available, those being interpolated to match the specified parameters. Although not very accurate, this method is much faster and allows a fast rough determination of the spectra, which is useful for scans of the parameter space.

In this paper the second method is used and all channels with probability greater than 0.1% plus  $\gamma\gamma$  and  $\gamma Z^0$  have been considered in the signal prediction.

### Set 1

For the first set of parameters, the following spectrum for the  $\gamma$  rays arising from Galactic center is obtained. Here the flux is high and the  $\gamma$  lines are undistinguishable from the continuous hadronization spectrum.

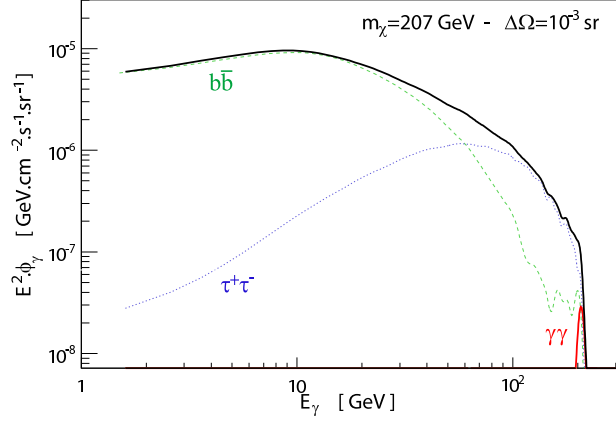


Figure 10:  $\gamma$  flux from Galactic center for set 1

### Set 2

For the second set of parameters, Figure 11 is obtained. As expected the flux is quite low but one can see very clearly the lines induced by  $\chi\chi \rightarrow \gamma\gamma$  and  $\chi\chi \rightarrow \gamma Z^0$ .

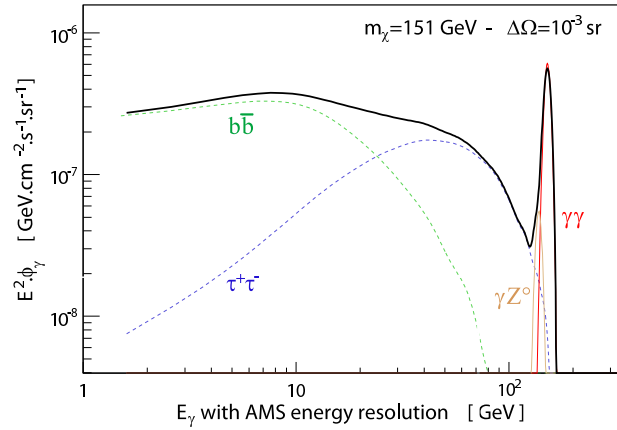


Figure 11:  $\gamma$  flux from Galactic center for set 2

Of course, those two spectra have to be added to the background and compared to AMS02 acceptance. According to the background expectation, it will be less obvious to extract the signal in the latter case (in next section a estimation of AMS02 sensitivity to this signal is presented). One can notice that the specific spectral features can only be observed with a very good energy resolution. In order to illustrate this, one can plot

the same spectrum with an typical Atmospheric Čerenkov Telescope (ACT) energy resolution, as it is done in Figure 12 (a  $\sim 30\%$  energy resolution is assumed).

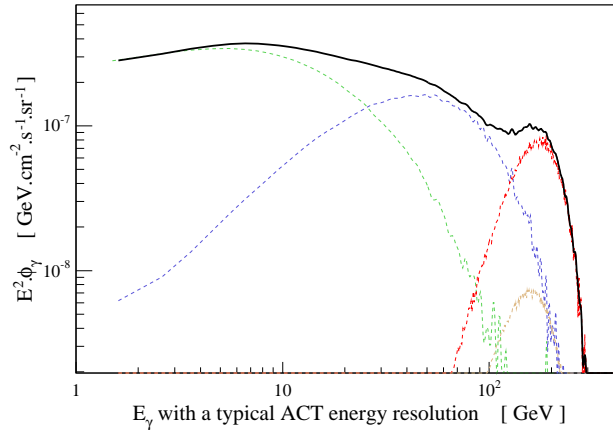


Figure 12: Same as previous Figure 11 with an ACT energy resolution

In the case of an ACT, the flux suppression at  $m_\chi$  could be seen, but the  $\gamma$  line itself is too much smeared by the energy resolution. Only a space mission like AMS02 would be able to do so.

### Estimation of theses fluxes observability with AMS02

As it was said before, the first set of parameters provides quite a high signal. In order to have a rough estimate of the observability of this flux with AMS02, an average acceptance of  $0.09 \text{ m}^2 \cdot \text{sr}$  is assumed, and the signal is integrated inside a solid angle of  $10^{-3} \text{ sr}$  corresponding to the  $1^\circ$  angular resolution of the Ecal. For 3 years of data taking, the measurement of the  $\gamma$  flux in case of set 1 would lead to the points of Figure 13. Here the expected background is a power law of spectral index 2.72 extrapolated out of the EGRET measurement of  $\gamma$  rays from the Galactic center region [18].

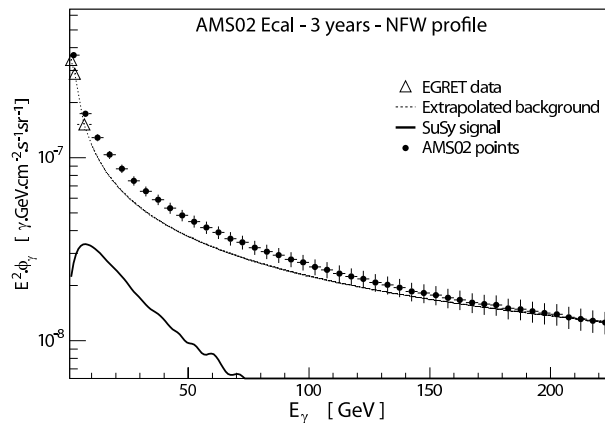


Figure 13: AMS02 measurement of the flux from Galactic center for set 1

In the second scenario, the signal shown on Figure 11 gives a signal that leads to an excess at the level of less than  $1\sigma$  over the background, even in 10 years of data taking. It would be possible to observe this line if the dark matter halo were more cusped than a typical NFW profile. In Figure 14, the observation of the line by AMS02 in 3 years is presented under the more optimistic assumption of a central cusp of index  $\gamma = 1.25$ .

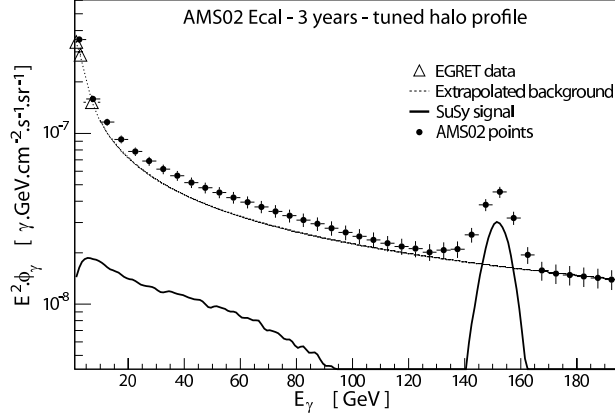


Figure 14: AMS02 measurement of the flux from Galactic center for set 2, with a specific halo profile

## 5 Second example : positron signal in AMSB

In the AMSB scenario, the neutralino is a pure wino, and the annihilation cross section is always higher than in the mSUGRA case. This has two main implications :

- The thermal relic density is very small so that one has to assume non thermal  $\chi$  production. Such a non-thermal relic density can be caused by non-standard cosmology [19] or decays of gravitinos produced at the end of inflation [20].
- The  $\chi\chi \rightarrow W^+W^-$  channel is always dominant as soon as it is kinematically allowed.

The annihilation into W bosons gives harder  $e^+$  signal than in the typical  $b\bar{b}$  case of mSUGRA. That is why this framework has been chosen to illustrate the generation of positron signal. In the example here, the SPS9 benchmark point [21] is used, for which :

SPS 9
$m_0 = 450 \text{ GeV}, m_{3/2} = 60 \text{ TeV}, tg(\beta) = 10, \mu > 0$
$(\Omega_\chi h^2)_{thermal} = 0.0018$
$m_\chi = 197.6 \text{ GeV}$
$\langle \sigma_{tot} v \rangle = 1.93 \cdot 10^{-24} \text{ cm}^3 \text{ s}^{-1}$
$\langle \sigma(W^+W^-) v \rangle = 0.991 \times \langle \sigma_{tot} v \rangle$
$\langle \sigma(\gamma\gamma) v \rangle = 0.0021 \times \langle \sigma_{tot} v \rangle$
$\langle \sigma(\gamma Z^0) v \rangle = 0.0065 \times \langle \sigma_{tot} v \rangle$

Figure 15: Main features of the SPS9 set of parameters

For the flux calculation, the same halo model as above is used. Figure 16 shows the  $e^+$  before propagation and after propagation. The code that was used here is currently under development [14] and its final version

will be implemented in `micrOMEGAs`. It makes use of a new positron propagator for the diffusion in the galaxy and its spatial resolution should not be limited, in order to allow the study of small dark matter structures. However for the signal shown here, the  $e^+$  source term is integrated over the whole galactic halo, taken to be smooth.

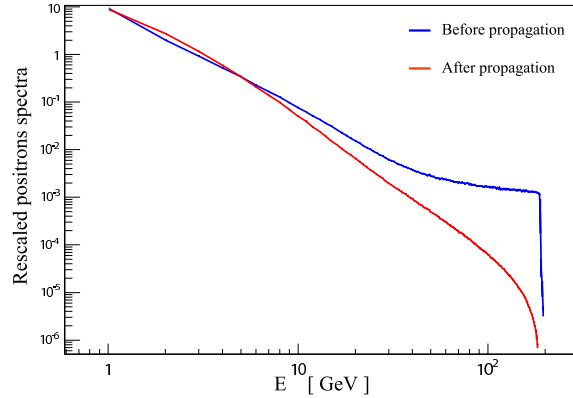


Figure 16: Positron source term and flux after propagation (see text)

Figure 16 shows the superimposition of the  $e^+$  source term (blue curve) and the flux after propagation. Here the red curve has been re-scaled in order to see the spectrum distortion due to propagation. The scale on the left corresponds to the source term in units  $positrons.GeV^{-1}$ . The scaling factor used here to draw the flux curve is of order  $10^6 cm^2.s.sr$ . Dark matter substructures (clumps) are awaited to produce an enhancement of the signal [14]. Because of the high annihilation cross-section and the specific high energy features of the W-induced positrons, a boost factor of only order unity is required to fit the HEAT positrons excess [7]. Figure 17 shows the SuSy signal in term of positron fraction, compared to the HEAT excess. The expected background is taken from [22].

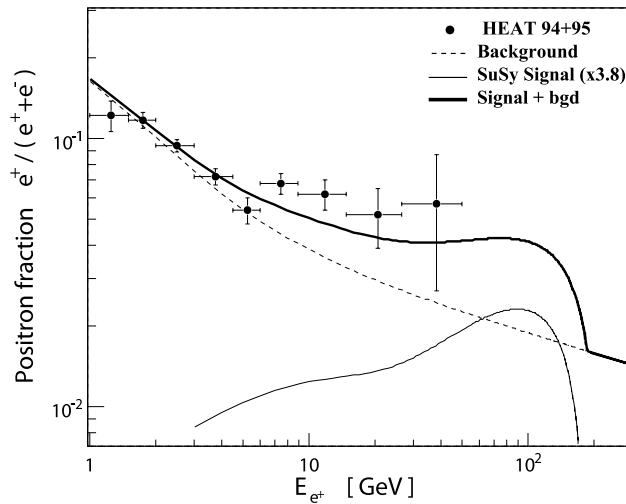


Figure 17: Fit to the HEAT data in AMSB

In Figure 17 the supersymmetric signal is multiplied by a factor of 3.8, this figure is to be compared to the typical mSUGRA case, in which the boost factor can vary from 10 to over 1000. An important feature of the AMSB scenario is the charginos/neutralinos mass degeneracy, which implies a very low sensitivity for hadron colliders to this model. Therefore if AMSB is the proper description of high energy physics, AMS02 would be in a very good position to observe SuSy.

## 6 Other charged channels : antiprotons and antideuterons

For the moment, the propagation of  $\bar{p}$  and  $\bar{D}$  is not implemented in the code. However, the injection spectra that stands for the source terms in the propagation equations are available. Figure 18 shows the source terms for these two channels.

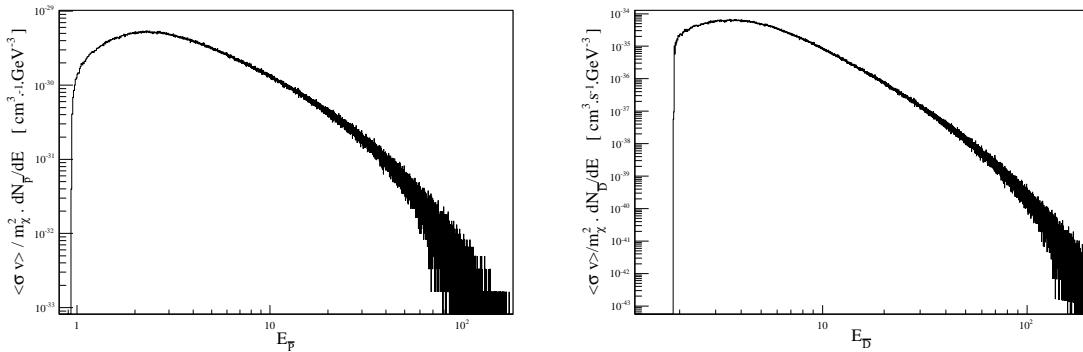


Figure 18:  $\bar{p}$  and  $\bar{D}$  source spectra

The  $\bar{D}$  spectrum is computed according to the coalescence model, see ref [23]. The adjunction of these channels in the code is currently under way.

## 7 Conclusions and outlook

In this note I gave some examples of SuSy signals which could be seen by AMS02. These illustrations show the potential of the package we are developing. Its possibilities will be even greater than what is shown here, it allows to work in any SuSy model and with any halo profile. In the final version, substructures and extragalactic sources studies will also be possible. Some comparisons with the only existing similar tool DarkSUSY [24] are being performed and we are currently working on the implementation of the  $\bar{p}$  and  $\bar{D}$  propagation. In the near future, the nature of dark matter could be unveiled by the spectral features of the annihilation signals in the Milky Way. Once published, this package could be a powerful tool for data analysis of all experiments performing indirect searches of dark matter.

## Acknowledgements

I would like to thank all the members of LAPP and LAPTH involved in this project for this fruitful and pleasant collaboration, as well as all the French working groups GDR SUSY and PCHE members.

## References

- [1] G. Bertone, D. Hooper, J. Silk, J., 2005, Phys. Rep., 405, 279
- [2] D.N. Spergel, *et al*, 2003, Astrophys. J. Supp., 148, 175
- [3] G. Bélanger, F. Boudjema, A. Pukhov, A. Semenov, 2002, Comp. Phys. Com., 149, 103, *ibid* [arXiv:hep-ph/0405253]
- [4] P. Binetruy, G. Girardi, P. Salati, 1984, Nucl. Phys. B, 237, 285
- [5] L. Randall, R. Sundrum, 1999, Nucl. Phys., B557, 79-118
- [6] J. Alcaraz, *et al*, 2002, Nucl. Instrum. Meth. A, 478, 119
- [7] J.J. Beatty, *et al.*, 2004, Phys. Rev. Lett., 93, 241102
- [8] J. Pochon, 2005, PhD thesis LAPP-T-2005-04
- [9] P. Brun, S. Rosier-Lees, 2005, AMS note 2005-01-12
- [10] L. Girard, 2004, PhD thesis LAPP-T-2004-05 and Proceedings of Moriond 2004
- [11] G. Bélanger, F. Boudjema, P. Brun, A. Pukhov, S. Rosier-Lees, P. Salati, 2006, *in preparation*
- [12] A. Djouadi, J.L. Kneur, G. Moultaka, G., 2002, [arXiv:hep-ph/0211331]
- [13] T. Sjöstrand, *et al.*, 2001, Comp. Phys. Com., 135, 238
- [14] J. Lavalle, J. Pochon, P. Salati, R. Taillet, 2006, *in preparation*
- [15] F. Boudjema, A. Semenov, D. Temes, D., 2005, Phys. Rev. D, 72, 055024
- [16] W. de Boer, M. Herold, C. Sander, V. Zhukov, 2003, [arXiv:hep-ph/0309029]
- [17] M. Battaglia, *et al.*, 2004, Eur. Phys. J., C33, 273
- [18] H. Mayer-Hasselwander, *et al.*, 1998, Astron. Astrophys. 335, 161.
- [19] P. Salati, 2003, Phys. Lett. B, 571, 121
- [20] T. Moroi, L. Randall, 1999, Nuc. Phys. B, 570, 455-472
- [21] B.C. Allanach, *et al*, 2002, Eur. Phys. J. C, 25, 113-123
- [22] E.A. Baltz, J. Edsjo, 1999, Phys. Rev. D, 59, 023511
- [23] F. Donato, N. Fornengo, P. Salati, 2000, Phys.Rev. D, 62, 043003
- [24] P. Gondolo, J. Edsjo, P. Ullio, L. Bergstrom, M. Schelke, E.A. Baltz, 2004, JCAP, 0407, 008